

Glycosylation Affects both the Three-Dimensional Structure and Antibody Binding Properties of the HIV-1_{IIIB} GP120 Peptide RP135[†]

Xiaolin Huang,[‡] Joseph J. Barchi, Jr.,^{*,‡} Feng-Di T. Lung,[‡] Peter P. Roller,[‡] Peter L. Nara,[§] Jeff Muschik,[§] and Robert R. Garrity[§]

Laboratory of Medicinal Chemistry, Division of Basic Sciences, National Cancer Institute, Bethesda, Maryland 20892, and Vaccine Resistant Diseases Section, Division of Basic Sciences, Frederick Cancer Research and Development Center, National Cancer Institute, Frederick, Maryland 21702

Received February 18, 1997; Revised Manuscript Received June 19, 1997[⊗]

ABSTRACT: We have prepared glycosylated analogues of the principal neutralizing determinant of gp120 and studied their conformations by NMR and circular dichroism spectroscopies. The 24-residue peptide from the HIV-1_{IIIB} isolate (residues 308–331) designated RP135, which contains the immunodominant tip of the V3 loop, was glycosylated with both N- and O-linked sugars. The structures of two glycopeptides, one with an N-linked β -glucosamine (RP135_{NG}) and the other with two O-linked α -galactosamine units (RP135_{digal}), were studied by NMR and circular dichroism spectroscopies. Molecular dynamics calculations based on the NMR data obtained in water solutions were performed to explore the conformational substates sampled by the glycopeptides. The data showed that covalently linking a carbohydrate to the peptide has a major effect on the local conformation and imparts additional minor changes at more distant sites of partially defined secondary structure. In particular, the transient β -type turn comprised of the -Gly-Pro-Gly-Arg- segment at the “tip” of the V3 loop is more highly populated in RP135_{digal} than in the native peptide and N-linked analogue. Binding data for the glycopeptides with 0.5 β , a monoclonal antibody mapped to the RP135 sequence, revealed a significant enhancement in binding for RP135_{digal} as compared with the native peptide, whereas binding was reduced for the N-linked glycopeptide. These data show that glycosylation of V3 loop peptides can affect their conformations as well as their interactions with antibodies. The design of more ordered and biologically relevant conformations of immunogenic regions from gp120 may aid in the design of more effective immunogens for HIV-1 vaccine development.

The envelope glycoprotein of HIV-1¹ is the 160 kDa product of the *env* gene which is cleaved into two non-covalently associated subunits of 120 and 41 kDa (gp120 and gp41). gp120 binds to the CD4 molecule expressed on T-cells whereas gp41 mediates fusion of the virus to the cell membrane of the infected host cell. A high-resolution, three-dimensional conformational assignment of native gp120 has eluded structural biologists due to the size and complexity of the protein. This information is vital for understanding the role played by different gp120 domains during attachment and infection of T-cells or macrophages.

Although the full-length structure has not been solved, individual segments of the molecule have been synthesized and studied by X-ray crystallography and CD and NMR spectroscopies. One of the most widely studied segments among the group of conserved (C1–C5) and variable (V1–

V5) domains that make up the gp120 polypeptide is V3. This disulfide-bridged loop of ca. 35 amino acids affects both viral tropism and syncytia formation (Hwang et al., 1991) and is a critical determinant of viral fusion (Page et al., 1992). In addition, antibodies to several epitopes within the V3 loop from different viral strains possess neutralizing activity (Robert-Guroff, 1990; Gorny et al., 1993). One of these antibodies designated 0.5 β , which was raised to HIV-1_{IIIB} infected cells, mapped to a 24-residue sequence in the center of the loop and was shown to prevent viral fusion and syncytia formation (Rusche et al., 1988). This peptide, denoted RP135, spans residues Asn³⁰⁸–Gly³³¹ in the IIIB isolate of HIV-1. This area of the V3 loop has been referred to as the principal neutralizing determinant (PND). The center of this domain contains the highly conserved segment -Gly-Pro-Gly-Arg- which is considered the “immunodominant tip” of the loop.

The structures of complete V3 loops from the Haitian (Catasti et al., 1996), MN (Catasti et al., 1995), RF (Vranken et al., 1996), and Thailand isolates (Gupta et al., 1993), as well as truncated segments from MN (Chandrasekhar et al., 1991), hybrid peptides containing T-helper epitopes linked to PND sequences (de Lorimer et al., 1994; Vu et al., 1996), and small, cyclic V3 peptides (Tolman et al., 1993), have been studied by NMR spectroscopy. The consensus of these studies was that the -Gly-Pro-Gly-Arg- segment forms a transient β -type turn (primarily type II) which was previously predicted from secondary structure analysis of a panel of

[†] This work was supported by a grant from the AIDS Targeted Antiviral Research Program of the Office of the Director, NIH.

* Address correspondence to this author at the NCI, Building 37, Room 5C02, 37 Convent Drive, MSC 4255, Bethesda, MD 20892. Telephone: 301-402-3113. FAX: 301-402-2275. Email: barchi@helix.nih.gov.

[‡] Laboratory of Medicinal Chemistry, NCI.

[§] Vaccine Resistant Diseases Section, FCRDC.

[⊗] Abstract published in *Advance ACS Abstracts*, August 15, 1997.

¹ Abbreviations: HIV-1, human immunodeficiency virus type 1; AIDS, acquired immunodeficiency syndrome; NOE, nuclear Overhauser enhancement; dNM, deoxynorjirimycin; TFE, trifluoroethanol; mAbs, monoclonal antibodies; PBS, phosphate-buffered saline; HBTu, 2-(1*H*-benzotriazol-1-yl)-1,1,3,3-tetramethyluronium hexafluorophosphate; HOBt, 1-hydroxybenzotriazole; DIEA, diisopropylethylamine; Pmc, 2,2,5,7,8-pentamethylchroman-6-sulfonyl; BOC, *tert*-butyloxycarbonyl.

245 PND sequences (La Rosa et al., 1990). In addition, the complex structures of two different antibodies bound to peptide fragments from HIV-1_{MN} have been solved by X-ray crystallography (Rini et al., 1993; Ghiara et al., 1994). The study by Rini et al. showed that a synthetic peptide fragment adopted a β -strand-type II- β -turn conformation when bound to the Fab fragment of the isolate-specific mAb 50.1, whereas Ghiara et al. found an unexpected additional turn for the -Gly-Arg-Ala-Phe- sequence in the complex between a 24-residue peptide and the Fab fragment of another broadly neutralizing antibody, 59.1. The RP135 sequence was also studied by NMR in water and TFE solutions (Zvi et al., 1992) and in the presence of an Fab fragment of 0.5 β (Zvi et al., 1995a). In water, it was found to sample a random set of conformations although the conserved β -turn was observed along with a nascent helical structure in the C-terminal domain (Zvi et al., 1992). In a subsequent study, a model was proposed for the interaction of the peptide with the 0.5 β antibody, whereby at least 12 residues contacted the antibody surface with the -Gly-Pro-Gly-Arg- crest at the center of this segment (Zvi et al., 1995a,b). These and other studies (Ivanoff et al., 1991) confirmed that the integrity of this segment is a critical determinant for the infective properties of the virus.

A major impediment to structural studies of the intact protein is the complex and heterogeneous glycosylation pattern of gp120, where N-linked, complex and high-mannose carbohydrate chains (Feizi, 1989; Leonard, 1990) along with a small number of O-linked glycans (Bernstein et al., 1993) comprise approximately 50% of the molecular weight of the protein. The structures and functions of the individual N-linked glycan chains of gp120 have been studied extensively and found to be associated with biological properties specific for this protein (Fenouillet & Jones, 1996; Benjouad et al., 1994; Fenouillet et al., 1990). Gruters et al. (1987) had shown that treatment of HIV-infected cultured lymphocytes with inhibitors of glucose-trimming enzymes (castanospermine, dNM) caused a loss of the cytopathogenic effects of virus on these cells. Completely deglycosylated protein retains its ability to bind and infect CD4⁺ T-cells, but the relative infectivity was reduced compared to the glycosylated form (Fenouillet et al., 1989). While N-linked sugars are not an absolute requirement for the interaction of gp120 with its cellular receptor on T-lymphocytes, the intact repertoire of glycans seems to be necessary for the creation of the functional disposition of the protein (Fenouillet & Jones, 1996) and for protecting the polypeptide from denaturation (Papandreou et al., 1996). The role of O-linked sugars is, as of yet, not clearly understood. However, gp120 carbohydrates have a powerful effect on the antigenicity of the protein. Monoclonal antibodies that neutralize virus have been shown to be dependent on the presence of particular N-linked sites within the protein (Trkola et al., 1996; Warriar et al., 1994). A more intriguing discovery was that mAbs to particular sugar structures present on either N- and O-linked sites have been shown to inhibit viral infection of various human T-cell lines (Hansen et al., 1990, 1991). In particular, antibodies to the Tn structure (*N*-acetylgalactosamine- α -Ser/Thr), an O-linked tumor-associated antigen expressed on primary and subtype carcinomas but rare in normal tissue, were found to neutralize virus and block fusion of HIV-infected cells with uninfected cells of both the lymphocytic and monocytoid origin (Hansen et al., 1990).

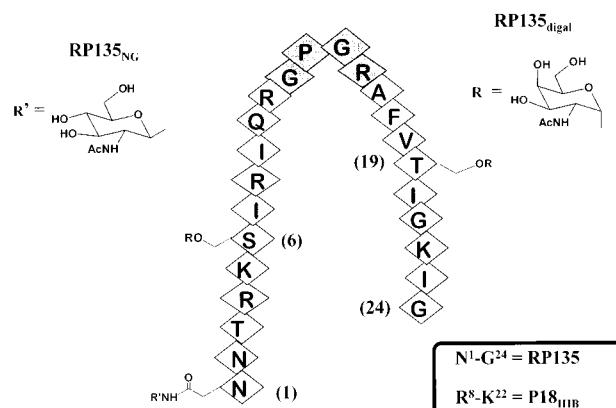


FIGURE 1: Structures of RP135, RP135_{digal}, and RP135_{NG}. HIV-1_{III B} V3 loop segment RP135 is shown with the crest of the loop (-Gly-Pro-Gly-Arg-) at the apex of the sequence. Residues Arg⁸-Lys²² constitute the P18 sequence (see text). Glycosylation sites are labeled.

Hence, carbohydrate epitopes, particularly GalNAc, may serve as alternative targets in the design of protective vaccines against the immunocompromising effects of HIV infection. Furthermore, since specific sugar epitopes may tend to be more broadly expressed among different isolates, immunization with a cocktail combining carbohydrate, peptide, and/or glycopeptide constructs could produce antibodies with the potential of being active against a wide variety of viral strains. However, only a limited number of structural studies have been done with gp120-derived glycopeptides (Laczko et al., 1992; Vuljanic et al., 1996; Markert et al., 1996).

Encouraged by our previous finding of the effects that simple O-glycosylation had on the structure and biological activity of a smaller peptide containing the tip of the V3 loop (Huang et al., 1996), we have now synthesized and studied the structures of glycosylated analogues of RP135 and compared these to the conformations proposed for the naked peptide sequence. The RP135 sequence contains the only N-linked glycosylation triplet (NXT/S, where X = any amino acid except proline or aspartic acid, Asn³⁰⁸, see Figure 1) located in the confines of the V3 loop itself, along with three potential O-linked sites (Thr³¹⁰, Ser³¹³, and Thr³²⁶). We have used the core sugar which is directly attached to the peptide backbone in natural glycoproteins, i.e., β -glucosamine (GlcNAc) and α -galactosamine (GalNAc) for the N- and O-linked glycopeptides, respectively, in the synthesis of glycosylated analogues of RP135 (Figure 1). The solution conformation of a digalactosylated analogue (RP135_{digal}) was shown to be significantly different from that of the unglycosylated RP135 or N³⁰⁸-glycosylated peptide (RP135_{NG}), particularly in the population of the turn structure surrounding the -Gly-Pro-Gly-Arg- crest. In addition, the RP135_{digal} construct bound to the 0.5 β antibody with a higher affinity than the unglycosylated sequence. This suggests that glycosylation affects both the conformation and the biological activity of immunologically significant peptides from the V3 region of gp120.

MATERIALS AND METHODS

Peptides. Peptides were synthesized by solid-phase synthesis using Fastmoc technology (HBTU, HOBt, and DIEA for activation) on an ABI 433A peptide synthesizer employing *N*-methylpyrrolidone as the washing solvent or manually

on PAL resin (Bachem). Protecting groups were as follows: arginine, Pmc; serine and threonine, *tert*-butyl; asparagine and glutamine, trityl; lysine, Boc. N^α -Fmoc- N^γ -(2-acetamido-2-deoxy-3,4,6-tri-*O*-acetyl- β -D-glucopyranosyl)-L-asparagine and N^α -Fmoc-*O*- β -(2-acetamido-2-deoxy-3,4,6-tri-*O*-acetyl- β -D-galactopyranosyl)-L-threonine were purchased from Oxford Glycosystems, and N^α -Fmoc-*O*- β -(2-acetamido-2-deoxy-3,4,6-tri-*O*-acetyl- β -D-galactopyranosyl)-L-serine was synthesized by a slight modification of a previously described route (Lüning et al., 1989). These glycosylated amino acids were incorporated into the peptides manually during the solid-phase synthesis. Coupling steps in the manual synthesis were run under similar activation conditions as those for the automated runs, specifically, 1.0 mL of 0.5 M HBTU, 0.5 mL of 1.0 M HOBt (solutions in DMF), and 0.091 mL of DIEA, plus 10 equiv of Fmoc-protected amino acids. Cleavage of the peptides from the resin was performed with a mixture of trifluoroacetic acid/thioanisole/water/ethanedithiol (10:0.5:0.5:0.25) for 2 h. The peptides were precipitated in ether, filtered, and purified by reverse-phase (C18) HPLC using a gradient of acetonitrile/water each containing 0.05% TFA. The acetate protecting groups on the sugar were removed by brief treatment with freshly prepared 1 M NaOMe in methanol at 0 °C. The products were repurified by C18 HPLC, affording pure glycosylated peptides as judged by FAB MS and NMR spectroscopy.

Circular Dichroism Spectroscopy and FAB Mass Spectrometry. CD spectra were recorded at room temperature in the wavelength range 190–260 nm, on a JASCO Model J-500A/DP501N spectropolarimeter, in Hellma QH cells with a path length of 1 mm. Peptide concentrations were 75 μ M in 10 mM phosphate buffer (pH 4.8 and 7.0), TFE, or TFE/buffer mixtures. The instrument was calibrated using an aqueous solution (60 mg/100 mL) of ammonium (1R)-(-)-10-camphorsulfonic acid (Aldrich Chemical Co.) using a 1 cm path length cell (negative maximum at 290.5 nm with an amplitude of -190.4 mdeg, $[Q]_{290.5} = -7910$ deg \cdot cm 2 ·dmol $^{-1}$). Mass spectra were recorded on a Finnegan MAT SSQ 7000 electrospray ionization mass spectrometer.

NMR Spectroscopy. Peptide samples were 6.7 mM dissolved in either 90% H₂O/10% D₂O, pure D₂O, or a mixture of 60% TFE/H₂O. All spectra were recorded on a Bruker AMX500 spectrometer at 5, 10, and 25 °C. The temperature was controlled by a Eurotherm control unit interfaced to a Bruker X32 computer. The pHs of the aqueous samples were adjusted to 4.8 with 10 mM phosphate buffer. The RP135_{digal} sample was also run at pH 2.9. DQF-COSY (Rance et al., 1983), TOCSY (Bax & Davis, 1985), ROESY (Bothner-By et al., 1985), and NOESY (Macura & Ernst, 1980) experiments were acquired with standard pulse sequences, and the water signal was suppressed by low-power presaturation during the relaxation delay and during the mixing time in the NOE experiments. TOCSY experiments were generally recorded with 2K data points and 32–64 scans per t_1 value while the NOE experiments were 64 scans per increment. The sweep width was 5050 Hz in each dimension for the homonuclear experiments. Mixing times of 250, 350, 400, and 600 ms were employed for the NOESY experiments and 350 ms for the ROESY data with a spin lock field of 2.5 kHz. 1 H– 13 C HMQC (Bax et al., 1983) spectra were recorded using a BIRD pulse to suppress magnetization of protons bound to 12 C. The sweep width in the carbon dimension was 175 ppm, and the 13 C 90° pulse

length was 14.7 μ s. Processing was performed on the X32 computer using shifted sine-bell apodization in both dimensions for the NOE data. All 2D spectra were baseline corrected with a polynomial of order 3 in both F_1 and F_2 . The data were transferred to a Silicon Graphics workstation where peak picking and calculation of peak volumes were done with NMRCOMPASS (Molecular Simulations Inc.). NOESY peak volumes were calculated from the spectrum collected with a 250 ms mixing time and were divided into three groups of strong (1.9–3.0 Å), medium (1.9–4.0 Å), and weak (1.9–5.0 Å), respectively. The temperature coefficients of the amide protons were studied by collecting TOCSY spectra at seven different temperatures between 5 and 35 °C in 5° increments and are reported in ppb/K.

Molecular Modeling and Structure Calculations. Model building and molecular dynamics simulations were performed on an SGI Indigo workstation in the context of the QUANTA molecular modeling package (version 4.1, Molecular Simulations, Inc.). The CHARMM force field (Brooks et al., 1983, version 23) was used for all calculations coupled either with QUANTA or with a stand-alone version on a DEC Alpha-Server 2100 (Digital Equipment Corp., Marlboro, MA). Carbohydrate parameters were taken from the POLY-SACCHARIDE.RTF residue topology file in CHARMM. Sugar residues were linked to the peptide backbone by a PATCH command in QUANTA. Energy minimization was typically computed until convergence (defined as an energy gradient of 0.001 kcal mol $^{-1}$ Å $^{-1}$), using the adopted basis Newton Raphson (ABNR) algorithm as implemented in CHARMM. Molecular dynamics simulations were carried out on structures either *in vacuo* using a distance-dependent dielectric constant ($D = r$) or in a system hydrated with a 10 Å sphere of preequilibrated water molecules. A shifted potential was used to a distance of 12 Å with a nonbonded cutoff of 14 Å. The nonbonded lists were updated every 25 steps of dynamics. A typical dynamics run was carried out by first heating the system from 0 to 300 K over 10 ps with a time step of 0.001 ps. The system was then equilibrated for 20 ps and a constant-temperature dynamics simulation was then performed for 100 ps. The simulation trajectory was recorded every 1 ps and subsequently analyzed to determine the behavior of the molecule. A SHAKE algorithm was used to constrain bonds to hydrogen to within 10 $^{-8}$ Å.

The restrained MD simulations were also carried out with a similar protocol as above, where the energy term for the distance restraints was added to the total potential energy of the system as a harmonic potential function. An iterative process was applied where additional NOEs were assigned from partially overlapped regions of the spectra based on the models generated from the simulations in water with unambiguous restraints. The best structures with lowest violation from this stage of the calculations were again energy minimized and subjected to restrained dynamic simulations at 278 K for 100 ps. The conformations with lowest violation and lowest energy were extracted on the basis of analyzing the final simulation trajectories.

Antibody Binding ELISAs. Details of this procedure are described elsewhere (Garrity et al., 1997). Briefly, Dynatec Immulon II 96-well ELISA plates were precoated with 100 μ L of a 1 mg/mL solution of peptides RP135, RP135_{digal}, or RP135_{NG} in 1 \times Dulbecco's PBS without CaCl₂ or MgCl₂ and incubated at 4 °C overnight. Plates were washed three

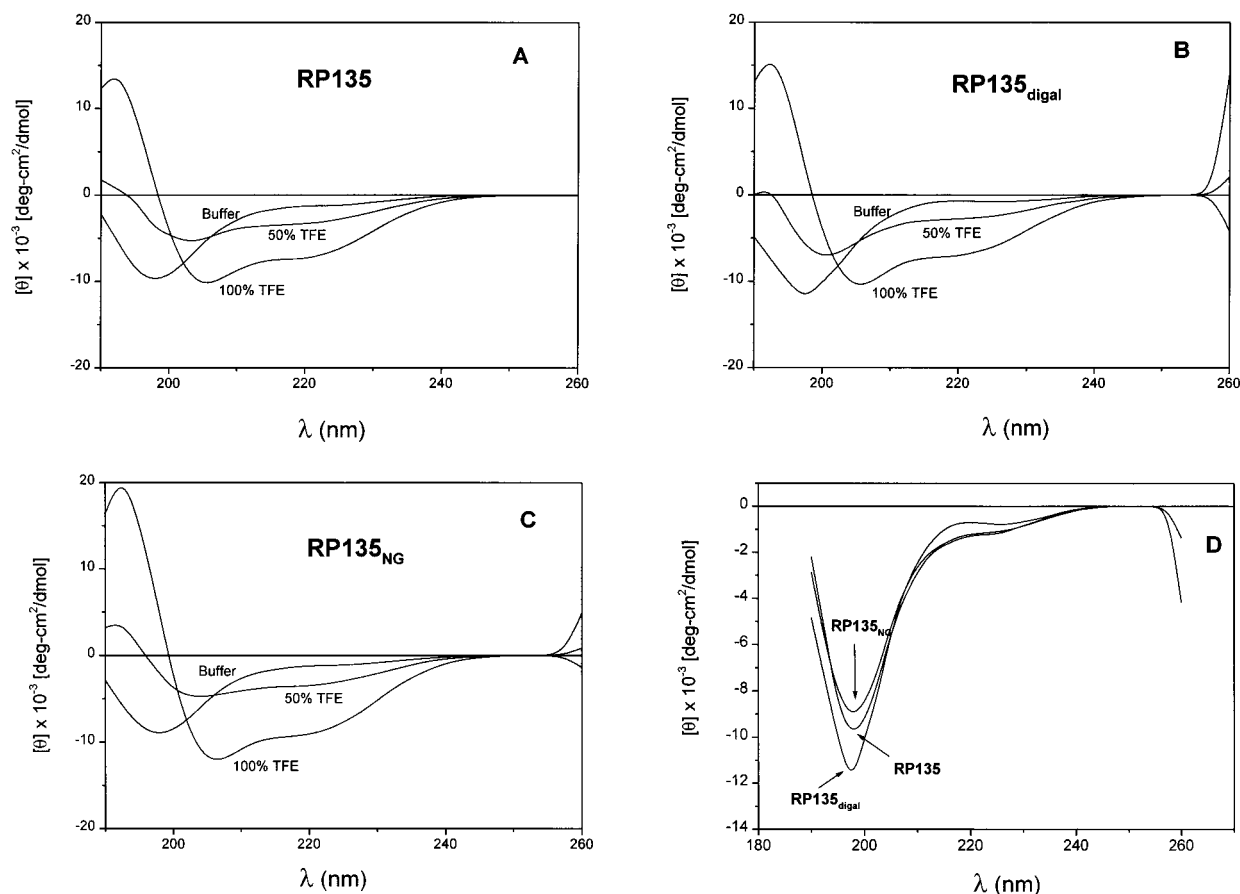


FIGURE 2: Circular dichroism spectra of RP135 (A), RP135_{digal} (B), and RP135_{NG} (C) in 10 mM phosphate buffer, 50% TFE/H₂O, and 100% TFE. Panel D shows the overlay of the buffer spectra of the three peptides.

times with 0.05% Tween 20 in sterile water to remove free peptide and blocked against nonspecific binding by incubation with 200 mL of 1% BSA for 30 min at 37 °C. After washing, 2-fold dilutions starting at 1:25 of 120 mg/mL primary 0.5 β mAb in PBS were allowed to bind for 1 h at 37 °C. Plates were washed three times and blocked against nonspecific binding by incubation with 200 mL of 10% sheep serum and 1% BSA solution for 30 min at 37 °C. After washing, 100 mL of a 1:1000 dilution of secondary sheep anti-mouse IgG–HRP was added to the plate, and the mixture was incubated at 37 °C for 1 h. After washing, color development was performed using *o*-phenylenediamine dihydrochloride substrate, and optical densities were determined at 492 nm by a Dupont Vmax plate reader.

RESULTS

Structural Characterization of Glycopeptides by Circular Dichroism. The CD spectra of the compounds used in the study are shown in Figure 2. A comparison of the spectra collected in varying amounts of 10 mM phosphate and TFE (panels A–C) are shown for each peptide along with an overlay of the traces of RP135, RP135_{NG}, and RP135_{digal} in 100% buffer (panel D). The shapes of the curves for all three of the peptides are generally similar whereas the absolute values of the molar ellipticities vary slightly among the analogues. Acquisition of additional secondary structure is evident in each peptide with an increase in solvent lipophilicity (panels A–C). In panel D, the traces are reminiscent of those observed in denatured proteins (random

coil). Curiously, RP135_{digal} exhibits the strongest negative band at 197 nm, indicative of a smaller proportion of secondary structure than RP135 and RP135_{NG}. However, it has been shown that spectra of this type may contain high percentages of β -turn (Johnson, 1988). As of yet, there are no established rules which explain the effect glycosylation has on the shape of the CD curves of peptides. Although the NMR structure of RP135_{digal} seems to be more well ordered than its unglycosylated counterpart (*vide infra*), a quantitative interpretation of the CD spectrum must await detailed analyses of the dichroic properties of various carbohydrates in the context of specific peptide sequences.

Structural Characterization of Glycopeptides by NMR Spectroscopy. NMR spectra of peptides RP135_{NG} and RP135_{digal} were collected at various conditions. Resonance assignments were made by established sequential strategy methods (Wüthrich, 1986). Assignment of the sugars was straightforward, starting with the well-resolved anomeric protons which resonate downfield of the water peak (Vliegenhart et al., 1983).

(A) Conformations in Water. A list of the chemical shifts of RP135_{NG} and RP135_{digal} is supplied in Tables 1 and 2, respectively. Figure 3 summarizes the NOEs observed in water solution for the N-glycosylated and digalactosylated peptides. In general, the peptides seem to be unordered in solution as was observed previously for RP135 (Zvi et al., 1992). However, glycosylation does have a decided effect on the structure and properties of these peptides. Relatively severe overlap of amide resonances was observed for each glycopeptide (Figures 4 and 5). However, the spectra of

Table 1: ^1H Chemical Shifts of RP135_{NG} in H₂O (pH = 4.8) at 5 °C

residue	NH	αH	βH	γH	others
Asn-1		4.347	2.984, 2.905		γNH 8.949
Asn-2	8.998	4.841	2.865, 2.786		γNH_2 7.049, 7.750
Thr-3	8.450	4.288	4.209	1.185	
Arg-4	8.544	4.308	1.847, 1.800	1.672	δCH_2 3.194; NH 7.246
Lys-5	8.553	4.308	1.804, 1.734	1.437	δCH_2 1.662; ϵCH_2 2.975; ϵNH_3^- 7.606
Ser-6	8.500	4.446	3.814		
Ile-7	8.386	4.189	1.838	1.442, 1.166	γCH_3 0.889; δCH_3 0.869
Arg-8	8.539	4.367	1.758, 1.620	1.521	δCH_2 3.171; NH 7.246
Ile-9	8.475	4.130	1.798	1.462, 1.166	γCH_3 0.875; δCH_3 0.850
Gln-10	8.697	4.347	2.035, 1.936	2.312	δNH_2 6.970, 7.645
Arg-11	8.648	4.387	1.837, 1.748	1.640	δCH_2 3.171; NH 7.246
Gly-12	8.475	4.140, 4.070			
Pro-13		4.426	2.270, 1.984	2.031	δCH_2 3.631
Gly-14	8.653	3.932			
Arg-15	8.278	4.268	1.787, 1.700	1.561	δCH_2 3.161; NH 7.220
Ala-16	8.426	4.249	1.284		
Phe-17	8.352	4.604	3.063, 3.004		(2,6)H 7.215; 4H 7.295; (3,5)H 7.330
Val-18	8.193	4.130	1.956	0.889	
Thr-19	8.430	4.327	4.110	1.195	
Ile-20	8.440	4.149	1.838	1.482, 1.186	γCH_3 0.909; δCH_3 0.850
Gly-21	8.613	3.913			
Lys-22	8.278	4.328	1.804, 1.734	1.373	δCH_2 1.662; ϵCH_2 2.978; ϵNH_3^+ 7.606
Ile-23	8.480	4.209	1.838	1.580, 1.185	γCH_3 0.908; δCH_3 0.850
Gly-24	8.294	3.779, 3.689			
N-NAG	8.347	1H 5.058	2H 3.813	3H 3.596	4H 3.497; 5H 3.525; 6H 3.767; COCH ₃ 1.996

Table 2: ^1H Chemical Shifts of RP135_{digal} in H₂O (pH = 4.8) at 5 °C

residue	NH	αH	βH	γH	others
Asn-1		4.339	2.975		
Asn-2	8.992	4.865	2.876, 2.797		γNH_2 7.046, 7.738
Thr-3	8.405	4.280	4.220	1.197	
Arg-4	8.506	4.319	1.790, 1.651	1.513	δCH_2 3.193; NH 7.268
Lys-5	8.503	4.304	1.792, 1.750	1.434	δCH_2 1.679; ϵCH_2 2.975; ϵNH_3^+ 7.608
Ser*-6	8.709	4.615	3.884, 3.726		
Ile-7	8.516	4.22	1.826	1.454, 1.156	γCH_3 0.881; δCH_3 0.843
Arg-8	8.604	4.367	1.730, 1.612	1.513	δCH_2 3.183; NH 7.268
Ile-9	8.521	4.102	1.806	1.485, 1.177	γCH_3 0.861; δCH_3 0.836
Gln-10	8.697	4.359	2.046, 1.948	2.323	δNH_2 6.967, 7.659
Arg-11	8.656	4.378	1.849, 1.750	1.631	δCH_2 3.173; NH 7.248
Gly-12	8.501	4.147, 4.042			
Pro-13		4.438	2.264, 1.987	2.030	δCH_2 3.627
Gly-14	8.634	3.924			
Arg-15	8.289	4.280	1.770, 1.691	1.552	δCH_2 3.153; NH 7.213
Ala-16	8.422	4.260	1.296		
Phe-17	8.331	4.635	3.094, 3.015		(2,6)H 7.235; 4H 7.286; (3,5)H 7.325
Val-18	8.210	4.260	1.987	0.920	
Thr*-19	8.733	4.576	4.260	1.256	
Ile-20	8.447	4.145	1.834	1.488, 1.206	γCH_3 0.940; δCH_3 0.876
Gly-21	8.560	4.003, 3.756			
Lys-22	8.439	4.299	1.750, 1.792	1.417	δCH_2 1.679; ϵCH_2 2.975; ϵNH_3^+ 7.608
Ile-23	8.447	4.141	1.860	1.510, 1.217	γCH_3 0.919; δCH_3 0.874
Gly-24	8.772	3.957, 3.865			
S-NAG	8.057	1H 4.853	2H 4.141	3H 3.805	4H 3.904; 5H 3.817; 6H 3.727, 3.728; COCH ₃ 2.027
T-NAG	7.850	1H 4.774	2H 4.062	3H 3.845	4H 3.944; 5H 4.019; 6H 3.785; COCH ₃ 2.007

RP135_{digal} (Figure 4) were more resolved than the RP135_{NG} peptide (Figure 5), suggesting that the diglycosylated structure is more ordered in solution than the N-terminal glycosylated peptide. Sequential NOE connectivities between H $_{\alpha}$ of Gly¹² and the H $_{\delta}$ protons of Pro¹³ indicated that the Gly-Pro bond in both glycopeptides was in the *trans* configuration.

Although a large number of $d_{\text{NN}}(i, i + 1)$ and strong consecutive $d_{\alpha\text{N}}(i, i + 1)$ correlations were observed throughout the sequences of both peptides, there was no evidence of $d_{\alpha\text{N}}(i, i + 3)$ or $d_{\alpha\beta}(i, i + 3)$ or longer range noncontiguous NOEs. These results indicate that the peptides do not show any preference for ordered helices or β -sheet motifs under these conditions. Both $d_{\text{NN}}(i, i + 1)$ and $d_{\alpha\text{N}}(i, i + 1)$ NOEs

are expected for peptides fluctuating between different backbone conformations (Dyson & Wright, 1991). Whereas the peptides show no strong preference for known secondary structural folds, the propensity to form a β -type turn around the conserved -GPGR- crest of the V3 loop was evident in both peptides. At 5 °C both RP135_{NG} and RP135_{digal} displayed characteristic NOEs around these residues, indicative of a β -type II turn [strong $d_{\text{NN}}(i, i + 1)$ between Gly¹⁴ and Arg¹⁵, strong $d_{\alpha\text{N}}(i, i + 1)$ between Pro¹³ and Gly¹⁴, and weak $d_{\alpha\text{N}}(i, i + 2)$ correlations between Pro¹³ and Arg¹⁵ (Figures 4 and 5)]. A very weak interaction between Pro¹³-H $_{\delta}$ and Gly¹⁴-NH suggested that a small population of a reverse turn of type I was also present in solution. These results are consistent with previous data on the NMR

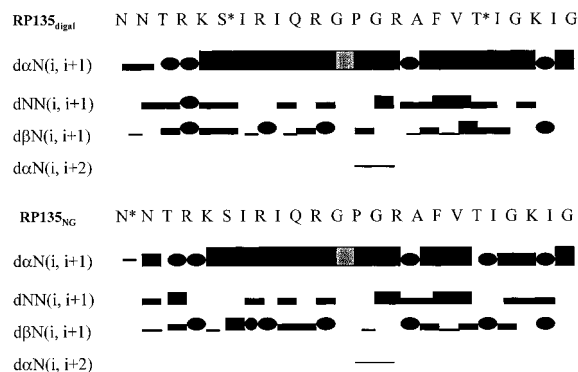


FIGURE 3: Schematic representation of the NOEs observed for the glycopeptides RP135_{digal} and RP135_{NG}. The thickness of the bars indicates the intensity of the correlation.

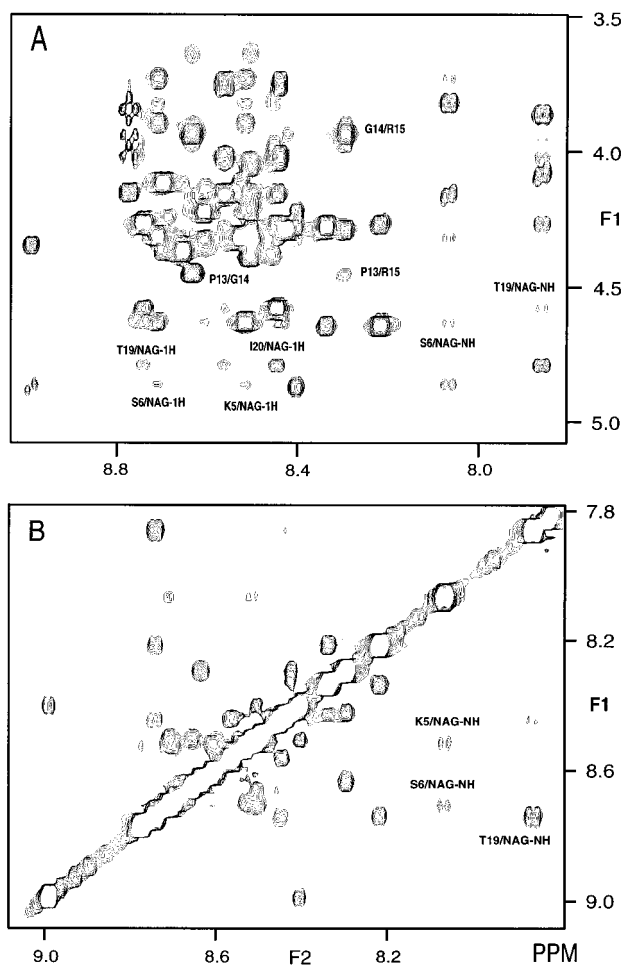


FIGURE 4: NOESY spectrum (300 ms mixing time) of the fingerprint and NH–NH regions of RP135_{digal} (A and B). Relevant peaks are labeled. The *N*-acetylgalactosamine units are abbreviated NAG.

structures of V3 loop peptides. Most intriguing was the behavior of the two peptides as the temperature was raised to 10 °C. The diagnostic $d_{\alpha N}(i, i + 2)$ NOE for the -Gly-Pro-Gly-Arg- turn in RP135_{NG} disappeared but was still evident by careful analysis of RP135_{digal}. Since characteristic peaks for a type II β -turn in previous NMR studies of different V3 loop peptides (Vranken et al., 1996; Chandrasekhar et al., 1991; de Lorimer et al., 1994; Vu et al., 1996) including the unglycosylated RP135 (Zvi et al., 1992) were observed only at 5 °C, our results confirm the stabilizing effect of the sugar moieties on the secondary structure of the

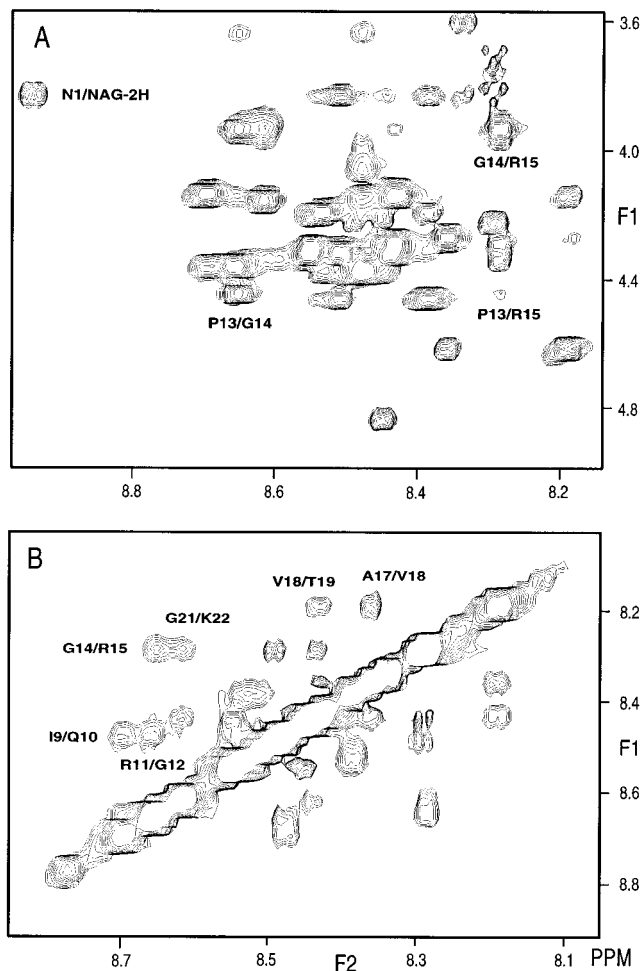


FIGURE 5: NOESY spectrum (300 ms mixing time) of the fingerprint and NH–NH regions of RP135_{NG}. Relevant peaks are labeled. The *N*-acetylglucosamine unit is abbreviated NAG.

peptide. Comparison of the data observed for RP135_{digal} with the 15-residue, galactosylated P18_{IIIb-g} peptide (Figure 1) we studied previously (Huang et al., 1996) shows that under identical conditions, the correlations are stronger in the longer sequence evident by stronger $d_{\alpha N}(i, i + 2)$ NOE interactions between Pro¹³ and Gly¹⁴ which may argue that flanking the turn with O-glycosylation sites has a somewhat “additive” effect on the disposition of the turn in solution. The details of the NMR structural evaluation around -Gly-Pro-Gly-Arg- for the RP135_{NG} sequence confirmed that the turn was only observed at 5 °C.

(B) *Temperature Coefficients.* Amide temperature coefficients were studied by collecting a series of TOCSY experiments at different temperatures (see Materials and Methods). Values of 7.4–10.4 ppb/K were observed for RP135_{NG} and 7.0–13.3 ppb/K for RP135_{digal}, indicating that no definitive hydrogen bonds or solvent-shielded amide resonances are present under the experimental conditions. These large values are surprising in light of the fact that the turn structure in the -Gly-Pro-Gly-Arg- crest seems to be populated in this medium. There is evidence, however, that the presence of reverse turns is not always contingent on a defined hydrogen bond between the *i*th residue CO and the amide of *i* + 3 (Rose et al., 1985). Relative to the rest of the sequence, the residues exhibiting the smallest coefficients were Arg¹⁵ and Val¹⁸, whose values were 7.75, 7.55 and 7.00, 7.13 for RP135_{NG} and RP135_{digal}, respectively.

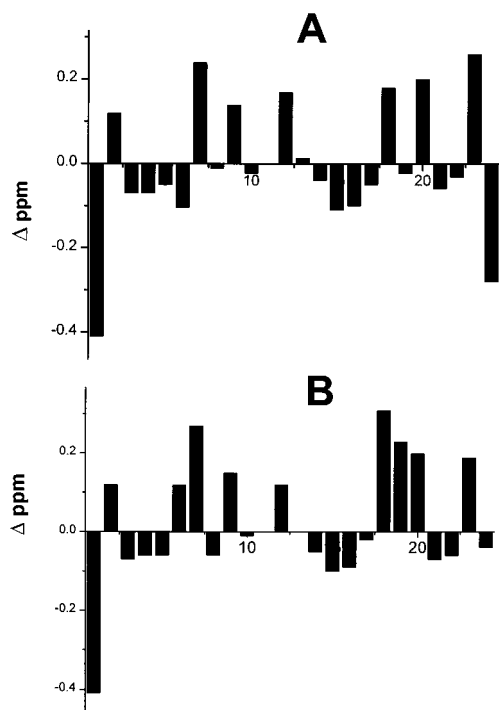


FIGURE 6: Chemical shift index maps of RP135_{NG} (A) and RP135_{digal} (B). Bars above the origin are C α protons which resonate downfield of random coil values, and bars below are those which resonate upfield of these values.

(C) *Conformation in TFE Solution.* Both CD and NMR studies were performed on the glycopeptides with the addition of various percentages of TFE. Salient features of the NMR of RP135_{NG} in 60% TFE/H₂O solution are summarized below. In comparison to the spectra in aqueous solution, stronger $d_{NN}(i, i + 1)$ and weaker $d_{\alpha N}(i, i + 1)$ connectivities were observed along with the additional medium-range $d_{\alpha N}(i, i + 2)$ correlations, viz., Gly¹²/Gly¹⁴, Ala¹⁶/Val¹⁸, Phe¹⁷/Thr¹⁹, Ile²⁰/Lys²², and Lys²²/Gly²⁴ (very weak). These data suggest that the conformers sampled by the C-terminal half of this glycopeptide in TFE solution have a preference for the α region of space (nascent helix). This is in accord with previous studies on similar constructs (Gupta et al., 1993). In contrast, the additional, medium-range correlations described above were not observed in the NMR spectra of RP135_{digal} in 60% TFE/H₂O, which suggested that the presence of the carbohydrate lowers the propensity to form helical structures in the vicinity of the glycosylation site.

A qualitative measure of the presence of secondary structure in peptides and proteins is the chemical shift index (CSI) of Wishart and Sykes (Wishart et al., 1992). These data are shown in Figure 6. An upfield shift with respect to empirically determined “random coil” values for the H α proton chemical shifts in a protein is indicative of a helical propensity for that residue whereas a downfield shift suggests a β -strand extended structure. The CSIs for RP135_{NG} (Figure 6A) and RP135_{digal} (Figure 6B) are similar with the exception of the chemical shifts of the glycosylated residues (6 and 19) and small deviations in the C-terminal residues between glycopeptides. Noteworthy are the indices for Val¹⁸-Thr¹⁹-Ile²⁰. In previous studies of the intact consensus V3 loop (Vranken et al., 1995), CSIs for the corresponding residues were negative, indicative of more helical character in this segment of the peptides. A positive CSI for these chemical

Table 3: Peptide-*N*-Acetylgalactosamine (NAG) NOEs from RP135_{digal}

NAG H ^a	peptide H	intensity	NAG H ^a	peptide H	intensity
H1	I ²⁰ NH	weak	NH	T ¹⁹ NH	strong
	T ¹⁹ CH ₃	strong		T ¹⁹ α H	weak
	T ¹⁹ α H	medium		T ¹⁹ β H	medium
	T ¹⁹ β H	strong		T ¹⁹ CH ₃	weak
	T ¹⁹ NH	very weak		V ¹⁸ CH ₃	weak
	G ²¹ NH	very weak		I ²⁰ NH	weak
	S ⁶ β H	strong		S ⁶ NH	medium
	S ⁶ α H	medium		K ⁵ NH	weak
	S ⁶ NH	very weak		S ⁶ α H	very weak
	K ⁵ α H	very weak		S ⁶ β H	very weak
H3	T ¹⁹ NH	very weak	-COCH ₃	T ¹⁹ NH	strong
	S ⁶ NH	very weak		G ²¹ NH	medium
	I ⁷ NH	very weak		I ²⁰ NH	weak
H5	T ¹⁹ CH ₃	strong		K ⁵ NH	very weak
				R ⁸ NH	very weak

^a NAG refers to the sugar bound to the Ser⁶ or Thr¹⁹ site for NOEs to residues Lys⁵-Arg⁸ or Val¹⁸-Gly²¹, respectively. Numbering is for RP135 (1-24).

shifts in RP135_{digal} (Figure 6B) suggests that the the aforementioned helical propensity in this region of the peptide is disrupted by O-glycosylation.

(D) *Sugar-Peptide Interactions.* Unlike RP135_{NG}, numerous enhancements were observed between the peptide backbone and the carbohydrates at each glycosylation site of RP135_{digal}. Table 3 lists the sugar-peptide NOEs for each glycosylation site and the intensity of the particular correlation. A total of 17 and 12 NOEs between carbohydrate protons and the peptide backbone were observed around the Thr¹⁹ and Ser⁶ glycosylation sites, respectively. From the large number of interactions observed, it was evident that the glycosidic torsion angles for the two sugars sample a preferred region of space around their respective sequences. This effective reduction in conformational flexibility has been demonstrated in several recent structural studies of O-linked glycopeptides (Andreotti & Kahne, 1993; Liang et al., 1995; Live et al., 1996; Urge et al., 1992; Lee, et al., 1996). As shown in Figure 5, stronger NOEs were observed around the Thr¹⁹ glycosylation site compared with the Ser⁶ site. For example, a strong NOE was observed between the amide proton of Thr¹⁹ and the *N*-acetyl group on galactosamine whereas the Ser⁶ NH and its covalently attached sugar amide proton displayed a weaker, albeit medium-strength NOE. The data suggest that there is more local rigidity around the Thr¹⁹ segment than near the Ser⁶ position, a result which is further supported by the molecular modeling (see below). However, a certain measure of “stability” is conferred on the neighboring residues around both sites. In contrast, the analysis of the RP135_{NG} structure showed that the only strong correlation to the sugar residue was between Asn¹ NH γ and the NAG-H2'. Weak NOEs were observed between Asn¹ NH γ /NAG-NH and Asn¹ H α /NAG-H1'. This showed that the amide linkage of the Asn¹ prefers to be fully extended with H2' of the glucosamine residue but does not interact with the peptide backbone.

Conformational Studies of Glycopeptides by Molecular Modeling. Calculations were carried out on these glycopeptides without initial restraints to examine the conformational space explored by each analogue. Compared to the N-linked glycopeptide RP135_{NG}, a higher proportion of β -turn-containing structures were sampled around the -Gly-

Pro-Gly-Arg- segment by RP135_{digal}, based on the analysis of the simulation trajectories. This suggests that the two O-linked sites stabilized the conserved turn motif in this peptide while simple N-terminal glycosylation has little, if any, structural effects. Restrained molecular dynamics studies with NOE-derived distance constraints were only performed on RP135_{digal} since the NOESY spectra of RP135_{NG} were similar to those observed for unglycosylated RP135. Analysis of the final restrained dynamics simulation trajectory for RP135_{digal} showed that all conformers fell into a stationary state after 10 ps of simulation; the total energies of respective conformers in the stationary state were within the fluctuation of $\pm 4\%$. Because of the limited proton-proton distance data available for these linear peptides, the simulated conformers showed relatively large variations in conformation. However, a well-defined local structure was observed around both glycosylation sites. Several structures were extracted which displayed the lowest restraint violations and energies. The depiction of the average structure from 20 final conformers is shown in Figure 7A. The β -turn is evident and well-defined in this glycopeptide.

Calculated depictions of the residues surrounding each glycosylation site in RP135_{digal} are shown in Figure 7B. In both the restrained and unrestrained calculations of the RP135_{digal} structures, the serine site exhibited more conformational mobility than the threonine site. The RMSD was 0.35 Å for the atoms included in the Val¹⁸-Thr¹⁹-Ile²⁰ sequence and slightly higher for the Lys⁵-Ser⁶-Ile⁷ site (0.41 Å). This is consistent with the NMR results in which different degrees of sugar-peptide interactions were observed for the two sites. Figure 7B shows that the galactosamine unit at the threonine site is in close contact with several peptide atoms whereas the galactosamine attached to Ser⁶ assumes a more apical position and the surrounding peptide backbone is distanced from the sugar, allowing more rotational freedom around the glycosidic bond. In a direct comparison with the shorter peptide P18_{IIB-g} (Huang et al., 1996, Figure 1) the RMSD for all backbone atoms for RP135_{digal} was 2.12 Å, which is 0.6 Å lower than the RMSD for the backbone atoms of P18_{IIB-g}. In addition, the RMSD of the -Gly-Pro-Gly-Arg- crest was reduced from 0.6 Å for P18_{IIB-g} to 0.4 Å for RP135_{digal}, providing additional proof that the two glycosylation sites in RP135_{digal} not only decrease the flexibility of the peptide structure overall but also have a remote effect on the -Gly-Pro-Gly-Arg- region.

Calculations of the glycosidic torsion angles for both sites revealed that the Thr¹⁹ site sampled a smaller range of torsion angles than the Ser⁶ site. The glycosidic torsion angles [ϕ is defined as H1-C1-O1-Thr-C β and ψ as C1-O1-(Thr)-C β -H β as defined by Vliegner et al. (1983)] sampled -40° to -62° and 26° to 40° for Ser(GalNAc) and Thr(GalNAc) ϕ angles, respectively, and -9° to 10° and -7° to -20° for Ser(GalNAc) and Thr(GalNAc) ψ angles, respectively, further confirming that the preferred space occupied by the rotation about the sugar-peptide linkage is very well defined in this system.

ELISA Assays for Antibody Binding. We have shown that O-linked glycosylation interacts locally with the peptide sequence and affects the secondary structure of the molecule. In order to further characterize the biological relevance of the attached sugars, the glycopeptides were tested for their binding to the 0.5 β mAb, and the data from triplicate ELISA assays are summarized in Figure 8. The graphs represent a

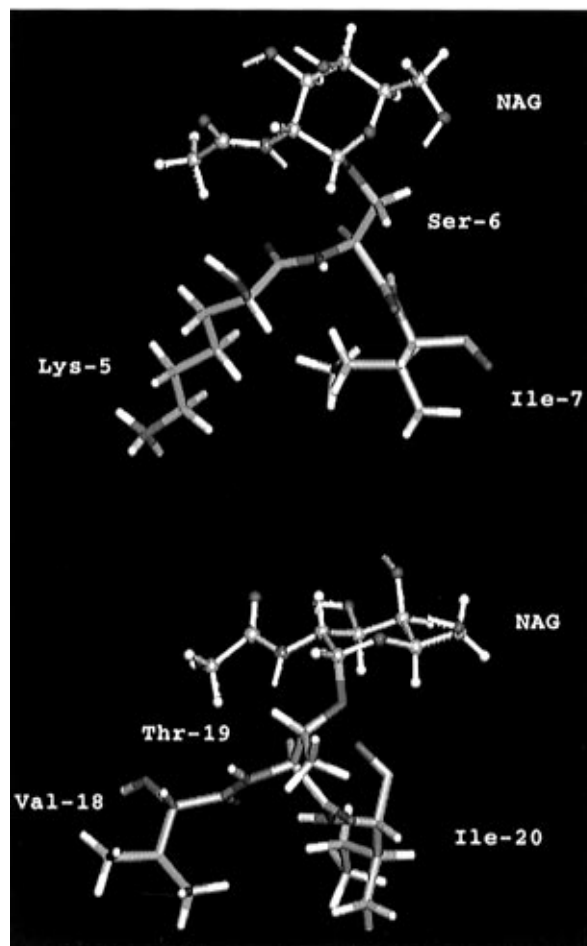
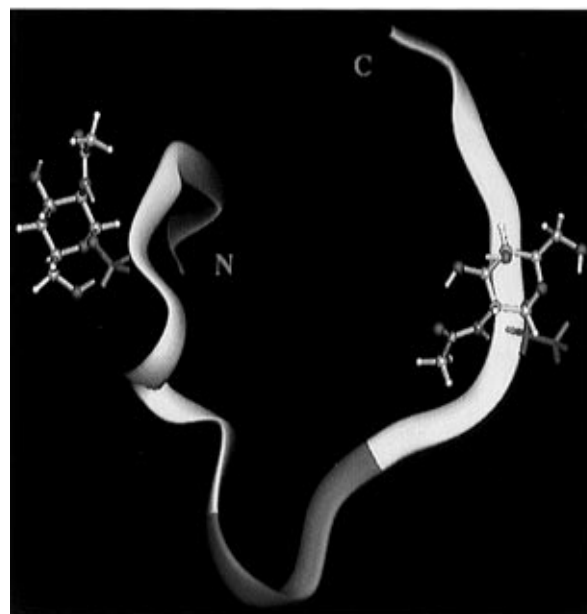


FIGURE 7: (A, top) Ribbon diagram of the best-fit average structure of RP135_{digal} from several molecular dynamics calculations in water based on NOE restraints using the protocol outlined in Materials and Methods. The sugar rings are shown in ball and stick representation, and the β -turn around the GPGR segment is shown in red. (B, bottom) Close-up rendering of the glycosylation sites from the calculated structure of RP135_{digal} shown in (A): Top, serine site; bottom, threonine site.

series of antibody dilutions which extend to a saturable (or near-saturable) end point. The bar graph (panel D) represents the optical densities for the 1:200 antibody dilution point of

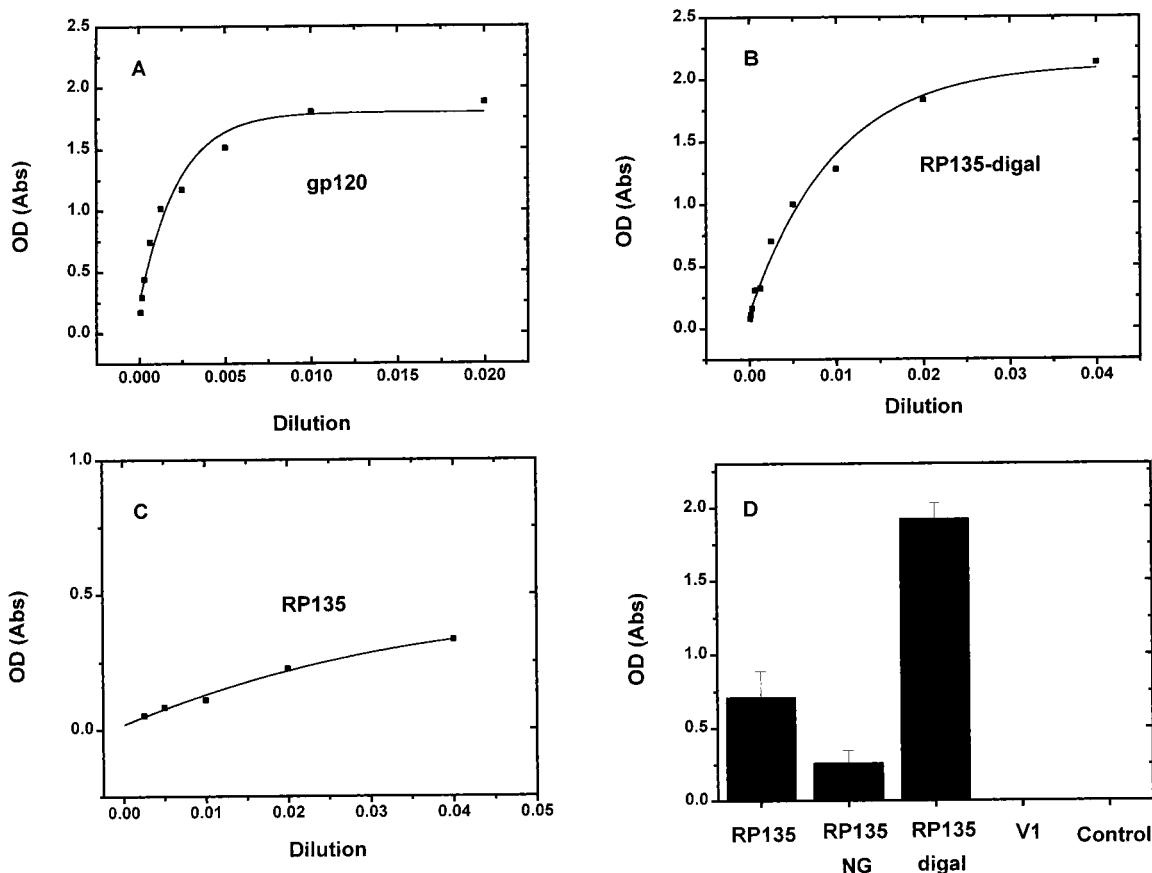


FIGURE 8: Results of ELISA antibody binding assays as described in Materials and Methods. Curves of optical density vs dilution⁻¹ are shown for binding of gp120 (A), RP135_{digal} (B), and RP135 (C). (D) Bar graph from the data of a 1:200 dilution of antibody. V1 is an additional control.

the test peptides. Comparisons were made to both the underivatized RP135 sequence and monomeric gp120. The data show that the diglycosylated construct bound the mAb not as well as gp120, but better by ~15-fold than the free RP135. Binding to 0.5 β was reduced slightly for the N-glycosylated peptide relative to RP135.

DISCUSSION

Glycosylation has been shown to have varying effects on the structure and function of small peptide models. With regard to peptide analogues from the V3 loop of gp120, previous studies have shown that mono- and disaccharides N-linked to an asparagine in small (8-residue) constructs from V3 had a stabilizing effect on the -Gly-Pro-Gly-Arg- β -turn as determined by CD and FT-IR spectroscopies (Laczko et al., 1992) while N-glycosylation with a single β -glucosamine (at the residue corresponding to N¹ in RP135) of complete, disulfide-bridged V3 loops from HIV-1 and HIV-2 subtypes did not affect the binding of these constructs to antisera from HIV-1 infected patients (Markert et al., 1996). In addition, glycosylation with *O*-galactosamine at the threonine C-terminal to the -Gly-Pro-Gly-Arg- crest (Thr¹⁹ in RP135) of a 17-residue peptide from V3_{IIB} did not have an effect on the backbone structure of the peptide as determined by limited NMR studies (Vuljanic et al., 1996). The present work shows that a significant conformational stabilization and modulation of binding properties can be achieved by simple *O*- α -galactosamylation of a highly immunogenic sequence of gp120. Mono-N-glycosylation did not have a significant effect on the structure or binding properties of

the peptide, our results being consistent with the work of Markert et al. (1996).

The studies where V3 constructs were explored by NMR or X-ray crystallography all suggest a reverse turn in the segment which includes -Gly-Pro-Gly-Arg-. The two crystal structures where an antibody which recognizes this portion of the loop was complexed to a peptide from the MN strain [mAb 50.1 (Rini et al., 1993) and mAb 59.1 (Ghiara et al., 1994)] both showed that the -Gly-Pro-Gly- segment adopts a turn-like conformation in the bound peptides. However, in the study by Ghiara et al., a second turn motif is observed which includes residues -Gly-Arg-Ala-Phe- leading to a double turn or "S"-like disposition of the six residues at the tip of the loop. Although the V3 loop from the MN strain lacks the dipeptide insert corresponding to Gln¹⁰-Arg¹¹ in RP135, the complex structure of mAb 59.1 with the peptide RP142 (Ghiara et al., 1994) demonstrates that these residues would not interact with 59.1. Hence, this mAb neutralizes a broad range of isolates including HIV_{IIB}. The majority of the bonded and nonbonded contacts made with 59.1 originate from the highly conserved Gly-Pro-Gly-Arg-Ala-Phe segment, implying that small, constrained molecules which position these moieties in the proper orientation may be useful as more broadly neutralizing immunogens or inhibitors of viral fusion (Ghiara et al., 1994). In fact, a very recent study by the same group showed that replacement of the alanine in this sequence by α -aminoisobutyric acid restricts the conformational flexibility of the peptide as demonstrated in both the solid and solution states (Ghiara et al., 1997).

In this study, we have stabilized this turn by simple, chemical modification with α -galactosamine. In effect, we have used a covalent attachment of a sugar as a conformational restraint, reminiscent of the constraints imposed by cyclization. A study by Tolman et al. (1994) showed that cyclic decapeptides which included the crown of the V3 loop from both the MN and IIIB strains could be used to raise broadly neutralizing antisera, but the authors caution that the data were inconsistent with the development of therapeutics from these constructs. We have shown that cyclo-(Gln-Arg-Gly-Pro-Gly-Arg-Ala-Phe) does not bind several mAbs specific for the crown of the IIIB V3 loop (Huang et al., unpublished). Both studies showed that the cyclic -Gly-Pro-Gly-Arg- segments assume type II β -turns. Thus, limiting the flexibility around this turn is not the sole requirement for antibody binding. These data, along with the information provided herein and that gleaned from the many NMR studies of V3 loop peptides, could provide a conceptual template for the structure-based design of small molecule inhibitors or potential immunogens that mimic the binding properties of RP135 or RP135_{digal}.

The interactions of peptides related to RP135 with 0.5 β have been studied by NMR spectroscopy. Studies employing NOE difference spectroscopy (Zvi et al., 1995b) and dynamic filtering (Zvi et al., 1995a) have shown that a segment of approximately 12 residues from RP135 interacts directly with a recombinant Fab fragment of the antibody. These 12 residues are those bordered by the glycosylated amino acids in RP135_{digal} (Ser⁶ and Thr¹⁹). How does glycosylation enhance the affinity of RP135_{digal} for the antibody? From the data available, it can be postulated that either the carbohydrate(s) is (are) interacting directly with the antibody combining site and contribute(s) to lower the energy of binding *via* additional hydrogen bonds or hydrophobic effects or the ensemble of conformations in solution for the RP135_{digal} glycopeptide presents a more favorable distribution of interacting residues (i.e., those enclosed by the glycosylation sites) to the antibody for proper docking. There is no direct evidence for any one postulate. However, the added stability of the -Gly-Pro-Gly-Arg- reverse turn and of the peptide itself imparted by the galactosamine groups in RP135_{digal} lead us to propose that glycosylation has adjusted the conformation of RP135 to more closely resemble the presentation of this epitope in the native protein. In contrast, the carbohydrate unit in RP135_{NG} is far removed from the critical segment of the epitope in contact with the antibody, and hence its behavior reflects that of the naked peptide. Our binding data suggest that, indeed, we have prepared a construct (RP135_{digal}) whose interaction with the mAb is similar to that shown by the intact protein (Figure 8). This method may be applied to indirectly determine the absence or presence of O-linked sites. The proposal that Thr¹⁹ was O-glycosylated in the native protein was originally made when a study by Clausen et al. (1993) showed that this threonine was enzymatically glycosylated when presented in the context of different V3 loop-derived peptides. However, the same group more recently presented data from site-directed mutagenesis and immunogenic mapping arguing against this proposal (Hansen et al., 1996). A more definitive answer must await additional research along these lines.

In conclusion, simple O-glycosylation was shown to have significant effects on the conformation of an important peptide epitope from the V3 loop by stabilizing a reverse

turn and rigidifying the backbone conformations proximal to the glycosylation sites. These structural adjustments resulted in an enhanced binding to a mAb which was raised to HIV-1_{IIIB}-infected cells and mapped to the unglycosylated epitope sequence. Studies such as this may be valuable in determining whether the presence of carbohydrates affects the three-dimensional conformation of gp120 subdomains. Additionally, covalently linked glycans may enhance epitope-specific antibody binding of these subdomains and prove useful in the design of glycopeptide-based vaccines.

SUPPORTING INFORMATION AVAILABLE

Two tables giving NMR distance restraints used in the dynamic simulation calculations and energies of several refined structures and one figure showing CD data at pH 7.0 on peptides RP135, RP135_{NG}, and RP135_{digal} (4 pages). Ordering information is given on any current masthead page.

REFERENCES

- Andreotti, A. H., & Kahne, D. (1993) *J. Am. Chem. Soc.* 115, 3352–3353.
- Bax, A., & Davis, D. G. (1985) *J. Magn. Reson.* 65, 355–360.
- Bernstein, H. B., Yucker, S. P., Huner, E., Schutzbach, J. S., & Compans, R. W. (1994) *J. Virol.* 68, 463–468.
- Brooks, B. R., Brucoleri, R. E., Olafson, B. D., States, D. J., Swaminathan, S., & Karplus, M. (1983) *J. Comput. Chem.* 4, 187–217.
- Brüenger, A. T. (1993) *X-PLOR Version 3.1: A System for X-ray Crystallography and NMR*, Yale University Press, New Haven, CT.
- Catasti, P., Fontenot, J. D., Bradbury, E. M., & Gupta, G. (1995) *J. Biol. Chem.* 270, 2224–2232.
- Catasti, P., Bradbury, E. M., & Gupta, G. (1996) *J. Biol. Chem.* 271, 8236–8242.
- Chandrasekhar, K., Profy, A. T., & Dyson, H. J. (1991) *Biochemistry* 30, 9187–9194.
- Clements, G. J., Price-Jones, M. J., Stephens, P. E., Sutton, C., Schulz, T. F., Clapham, P. R., McKeating, J. A., McClure, M. O., Thomson, S., Marsh, M., Kay, J., Weiss, R. A., & Moore, J. P. (1991) *AIDS Res. Hum. Retroviruses* 7, 3.
- Dedera, D., Vander Heyden, N., & Ratner, L. (1990) *AIDS Res. Hum. Retroviruses* 6, 785–794.
- de Lorimier, R., Moody, M. A., Haynes, B. F., & Spicer, L. D. (1994) *Biochemistry* 33, 2055–2062.
- Dyson, H. J., & Wright, P. E. (1991) *Annu. Rev. Biophys. Biophys. Chem.* 20, 519–538.
- Fast, P. E., & Walker, M. C. (1993) *AIDS* 7 (Suppl. 1), S147–159.
- Feizi, T., & Larkin, M. (1990) *Glycobiology*. 1, 17–23.
- Fenouillet, E., & Gluckman, J. C. (1991) *J. Gen. Virol.* 72, 1919–1926.
- Fenouillet, E., & Jones, I. M. (1996) *Prospectives in Drug Discovery and Design* 5, 203–212.
- Fenouillet, E., Clerget-Raslain, B., Gluckman, J. C., Guetard, U., Montagnier, L., & Bahraoui, E. (1989) *J. Exp. Med.* 169, 807–822.
- Fenouillet, E., Gluckman, J. C., & Jones, I. M. (1994) *Trends Biochem. Sci.* 19, 65–70.
- Fontenot, J. D., Gatewood, J. M., Santhana Mariappan, S. V., Pau, C.-P., Parekh, B. S., George, J. R., & Gupta, G. (1995) *Proc. Natl. Acad. Sci. U.S.A.* 92, 315–319.
- Garrity, R. R., Rimmelzwaan, G., Minassian, A., Tsai, W.-P., Liu, G., de Jong, J. J., Goudsmit, J., & Nara, P., (1997) *J. Immunol.* 159, 279–289.
- Gerken, T. A., Butenhof, K. J., & Shogren, R. (1989) *Biochemistry* 28, 5536–5543.
- Ghiara, J. B., Stura, E. A., Stanfield, R. L., Profy, A. T., & Wilson, I. A. (1994) *Science* 264, 82–85.
- Ghiara, J. B., Ferguson, D. C., Satterthwait, A. C., Dyson, H. J., & Wilson, I. A. (1997) *J. Mol. Biol.* 266, 31–39.

- Gorny, M. K., Xu, J.-Y., Giankakos, V., Karwowska, S., Williams, C., Sheppard, H. W., Hanson, C. V., & Zolla-Pazner, S. (1991) *Proc. Natl. Acad. Sci. U.S.A.* 8, 3238–3242.
- Goudsmit, J., Debouck, C., Meloen, R. H., Smit, L., Bakker, M., Asher, D. M., Wolff, A., Gibbs, C. J., Jr., & Gajdusek, D. C. (1988) *Proc. Natl. Acad. Sci. U.S.A.* 85, 4478–4482.
- Gruters, R. A., Neefjes, J. J., Tersmette, M., de Goede, R. E. Y., Tulp, A., Huisman, H. G., Miedema, F., & Ploegh, H. L. (1987) *Nature* 330, 74–77.
- Gupta, G., Anantharamaiah, G. M., Scott, D. R., Eldrige, J. H., & Meyers, G. (1993) *J. Biomol. Struct. Dyn.* 11, 345–366.
- Hansen, J.-E. S. (1992) *APMIS* 100, 96–108.
- Hansen, J.-E. S., Clausen, H., Nielsen, C., Teglbjærg, L. S., Hansen, L. L., Nielsen, C. M., Dabelsteen, E., Mathiesen, L., Hakomori, S.-I., & Nielsen, J. O. (1990) *J. Virol.* 64, 2833–2840.
- Hansen, J.-E. S., Hofmann, B., Pallesen, T., & Clausen, H. (1994) in *Complex Carbohydrates in Drug Research. 36th Alfred Benzon Symposium, 1993* (Bock, K., & Clausen, H., Eds.) pp 414–427, Copenhagen, Munksgaard.
- Hansen, J.-E. S., Jansson, B., Gram, G. J., Clausen, H., Nielson, J. O., & Olofsson, S. (1996) *Arch. Virol.* 141, 291–300.
- Huang, X., Smith, M. C., Berzofsky, J. A., & Barchi, J. J., Jr. (1996) *FEBS Lett.* 393, 280–286.
- Hwang, S. S., Boyle, T. J., Lyster, H. K., & Cullen, B. R. (1992) *Science* 253, 71–74.
- Imperiali, B., & Rickert, K. W. (1995) *Proc. Natl. Acad. Sci. U.S.A.* 92, 97–101.
- Ivanoff, L. A., Looney, D. J., Mcdanal, C., Morris, J. F., Wong-Staal, F., Langlois, A. J., Petteway, S. R., Jr., & Matthews, T. J. (1991) *AIDS Res. Hum. Retroviruses* 7, 595–603.
- Javaherian, K., Langlois, A. J., McDanal, C., Ross, K. L., Eckler, L. I., Jellis, C. L., Profy, A. T., Rusche, J. R., Bolognesi, D. P., Putney, S. D., & Matthews, T. J. (1989) *Proc. Natl. Acad. Sci. U.S.A.* 86, 6768–6772.
- Johnson, W. J., Jr. (1988) *Annu. Rev. Biophys. Biophys. Chem.* 17, 145–166.
- Jones, I., & Jacob, G. S. (1991) *Nature* 352, 198.
- Laczko, I., Hollósi, M., Úrge, L., Ugen, K. E., Weiner, D. B., Mantsch, H. H., Thurin, J., & Ötvös, L., Jr. (1992) *Biochemistry* 31, 4282–4288.
- Lee, K.-C., Falcone, M. L., & Davis, J. T. (1996) *J. Org. Chem.* 61, 4198–4199.
- Liang, R., Andreotti, A. H., & Kahne, D. (1995) *J. Am. Chem. Soc.* 117, 10395–10396.
- Live, D. H., Kumar, R. A., Beebe, X., & Danishefsky, S. J. (1996) *Proc. Natl. Acad. Sci. U.S.A.* 93, 12759–12761.
- Lüning, B., Norberg, T., & Tejbrant, J. (1989) *Glycoconjugate J.* 6, 5–19.
- Macura, S., & Ernst, R. R. (1980) *Mol. Phys.* 41, 95–117.
- Markert, R. L. M., Ruppach, H., Gehring, S., Dietrich, U., Mierke, D. F., Kock, M., Rubsam, W., Waigmann, H., & Griesinger, C. (1996) *Eur. J. Biochem.* 237, 188–204.
- Mascola, J. R., Snyder, S. W., Weislow, O. S., et al. (1996) *J. Infect. Dis.* 173, 340–348.
- Matthews, T. J., Weinhold, K. J., Lyster, H. K., Langlois, A. J., Wigzell, H., & Bolognesi, D. P. (1987) *Proc. Natl. Acad. Sci. U.S.A.* 84, 5424–5428.
- Meldal, M., & Bock, K. (1994) *Glycoconjugate J.* 11, 59–63.
- Nehete, P. N., Arlinghaus, R. B., & Sastry, K. J. (1993) *J. Virol.* 67, 6841–6846.
- Page, K. A., Stearns, S. M., & Littman, D. R. (1992) *J. Virol.* 6, 524–533.
- Palker, T. J., Clark, M. E., Langlois, A. J., Matthews, T. J., Weinhold, K. J., Randall, R. R., Bolognesi, D. P., & Haynes, B. F. (1988) *Proc. Natl. Acad. Sci. U.S.A.* 85, 1932–1936.
- Papandreou, M. J., Idziorek, T., Miquelis, R., & Fenouillet, E. (1996) *FEBS Lett.* 379, 171–176.
- Rance, M., Sorenson, O. W., Bodenhausen, G., Wagner, G., Ernst, R. R., & Wüthrich, K. (1983) *Biochem. Biophys. Res. Commun.* 117, 479–485.
- Rini, J. M., Stanfield, R. L., Stura, E. A., Salinas, P. A., Profy, A. T., & Wilson, I. A. (1993) *Proc. Natl. Acad. Sci. U.S.A.* 90, 635–6329.
- Robert-Guroff, M. (1990) *Int. Rev. Immunol.* 7, 15–30.
- Rose, G. D., Gierasch, L. M., & Smith, J. A. (1985) *Adv. Protein Chem.* 37, 1–106.
- Rusche, J. R., Javaherian, K., McDanal, C., Petro, J., Lynn, D. L., Grimaila, R., Langlois, A. J., Gallo, R. C., Arthur, L. O., Fischinger, P. J., Bolognesi, D. P., Putney, S. D., & Matthews, T. J. (1988) *Proc. Natl. Acad. Sci. U.S.A.* 85, 3198–3202.
- Steimer, K. S., Sakamoto, D., Sun, Y. D., West, D., Baenziger, J., & Sinangil, F. (1994) *J. Cell. Biochem.* 8B, 114.
- Tolman, R. L., Bednarek, M. A., Johnson, B. A., Leanza, W. J., Marburg, S., Underwood, D. J., Emini, E. A., & Conley, A. J. (1993) *Int. J. Pep. Protein Res.* 41, 455–466.
- Trkola, A., Purtscher, M., Muster, T., Ballaun, C., Buchacher, A., Sullivan, N., Srinivasan, K., Sodroski, J., Moore, J. P., & Katinger, H. (1996) *J. Virol.* 70, 1100–1108.
- Úrge, L., Gorbics, L., & Ötvös, L., Jr. (1992) *Biochem. Biophys. Res. Commun.* 184, 1125–1132.
- Vliegthart, J. F. G., Dorland, L., & Van Halbeek, H. (1983) *Adv. Carbohydr. Chem. Biochem.* 41, 209–374.
- Vranken, W., Budesinsky, M., Martins, J. C., Fant, F., Boulez, K., Gras-Masse, H., & Borremans, F. A. M. (1996) *Eur. J. Biochem.* 236, 100–108.
- Vu, H. M., de Lorimier, R., Moody, M. A., Haynes, B. F., & Spicer, L. D. (1996) *Biochemistry* 35, 5158–5165.
- Vuljanic, T., Bergquist, K.-E., Clausen, H., Roy, S., & Kihlberg, J. (1996) *Tetrahedron* 52, 7983–8000.
- White-Scharf, M. E., Potts, B. J., Smith, L. M., Sokolowski, K. A., Rusche, J. R., & Silver, S. (1993) *Virology* 192, 197–206.
- Wishart, D. S., Sykes, B. D., & Richards, M. F. (1992) *Biochemistry* 31, 1647–1651.
- Woody, R. W. (1995) *Methods Enzymol.* 246, 34–71.
- Wüthrich, K. (1986) *NMR of Proteins and Nucleic Acids*, John Wiley and Sons, New York.
- Zvi, A., Hiller, R., & Anglister, J. (1992) *Biochemistry* 31, 6972–6979.
- Zvi, A., Kustanovich, I., Feigelson, D., Levy, R., Eisenstein, M., Matsushita, S., Richalet-Secordel, P., Regenmortel, M. H. V., & Anglister, J. (1995a) *Eur. J. Biochem.* 229, 178–189.
- Zvi, A., Kustanovich, I., Hayek, Y., Matsushita, S., & Anglister, J. (1995b) *FEBS Lett.* 368, 267–270.

BI9703655